

ORIGINAL ARTICLE

The diagnostic value of a seven-autoantibody panel and a nomogram with a scoring table for predicting the risk of non-small-cell lung cancer

Weidong Wang  | Runzhou Zhuang | Honghai Ma | Likui Fang | Zhitian Wang | Wang Lv | Jian Hu 

Department of Thoracic Surgery, The First Affiliated Hospital, School of Medicine, Zhejiang University, Hangzhou, China

Correspondence

Jian Hu, Department of Thoracic Surgery, The First Affiliated Hospital, School of Medicine, Zhejiang University, 79 Qingchun Road, Hangzhou, Zhejiang 310003, China. Email: hujian_zju@126.com

Funding information

Major science and Technology Projects of Zhejiang Province, Grant/Award Number: 2014C03032; Key Disciplines of Traditional Chinese Medicine in Zhejiang Province, Grant/Award Number: 2017-XK-A33; National Key R&D Program of China, Grant/Award Number: 2017YFC0113500; National Natural Science Foundation of China, Grant/Award Number: 31700690

Abstract

The early detection of non-small-cell lung cancer (NSCLC) remains a common concern. The aim of our study was to validate the diagnostic value of a seven-autoantibody (7-AAB) panel compared with radiological diagnosis for NSCLC. We constructed a nomogram and a scoring table based on the 7-AAB panel's result to predict the risk of NSCLC. We prospectively enrolled 268 patients who presented with radiological lesions and underwent both the 7-AAB panel test and pathological diagnosis by surgical resection. A comparison between the 7-AAB panel and radiological diagnosis was performed. A nomogram and a scoring table based on the 7-AAB panel's result to predict the risk of NSCLC were constructed and internally validated. The 7-AAB panel test had a specificity of 90.2% and a positive predictive value (PPV) of 92.7%, which were significantly higher than those of the radiological diagnosis. The 7-AAB panel also showed a preferable sensitivity in patients with early-stage disease. Seven factors, including the 7-AAB panel results, were integrated into the nomogram. For more convenient application, we formulated a scoring table based on the nomogram. The area under the receiver operating characteristic curve was 0.840 and 0.860 in the training group and validation group, respectively, which was higher than that using the 7-AAB panel or radiological diagnosis alone. This study reveals that our 7-AAB panel has clinical value in the diagnosis of NSCLC. The utility of our nomogram and the scoring table indicated that they have the potential to assist clinicians in avoiding unnecessary treatment or needless follow-up.

KEYWORDS

autoantibodies, CT scanning, early diagnosis, nomogram, non-small-cell lung cancer

Abbreviations: AABs, autoantibodies; AIS, adenocarcinoma in situ; AUC, area under the curve; CFDA, China Food and Drug Administration; CTC, circulating tumor cell; ELISA, enzyme-linked immunosorbent assay; GGO, ground-glass opacity; LDCT, low-dose computed tomography; MIA, minimally invasive adenocarcinoma; NSCLC, non-small-cell lung cancer; PPV, positive predictive value; ROC, receiver operating characteristic; SCLC, small-cell lung cancer; SE, standard error; TAA, tumor-associated antigen.

This is an open access article under the terms of the Creative Commons Attribution-NonCommercial License, which permits use, distribution and reproduction in any medium, provided the original work is properly cited and is not used for commercial purposes.

© 2020 The Authors. *Cancer Science* published by John Wiley & Sons Australia, Ltd on behalf of Japanese Cancer Association.

1 | INTRODUCTION

According to the latest global cancer statistics, lung cancer is the malignant tumor with the highest morbidity and mortality worldwide.¹ Lung cancer is divided into small-cell lung cancer (SCLC) and non-small-cell lung cancer (NSCLC) for the purpose of treatment. The latter is the most common pathological pattern, accounting for over 80% of patient cases.² For NSCLC, the 5-y survival rate differs dramatically from 92% for patients with stage IA disease to less than 10% for patients with distant metastatic disease.³ Unfortunately, only approximately 20% of patients with NSCLC are diagnosed at an early stage (stages I and II), which causes the poor survival of patients with NSCLC worldwide. Therefore, it is urgent to detect, screen, and diagnose NSCLC at an early stage to improve the survival outcome of this malignancy.⁴

The National Lung Screening Trial Research Team reported that using low-dose computed tomography (LDCT) screening compared with chest X-ray can reduce lung cancer mortality by 20%, so LDCT is recommended in many authoritative guidelines.^{5,6} Another famous study, the NELSON study, also indicated that LDCT can improve the detection rate of lung cancer, especially in patients with stage I disease.⁷ However, the problem still remains. Although the sensitivity of LDCT screening is over 90%, the specificity is not satisfied because that more than half of patients' lesions are undetermined in preliminary radiological diagnosis, which leads to a high false-positive rate of 96.3% and unnecessary operation.^{8,9} Furthermore, the radiation exposure of repeated CT examination is also considered a carcinogenic factor. In addition, patients with adenocarcinoma in situ (AIS) or minimally invasive adenocarcinoma (MIA) only need sublobar resection, and the 5-y survival rate is approximately 100%; the imaging features are often nontypical and need follow-up. Repeated imaging can increase the psychological burden of patients and cause the disease to develop to an advanced stage with a worse prognosis. Therefore, a novel method should be developed to enhance the diagnostic value of CT screening to detect NSCLC at an early stage.

Serum autoantibodies (AABs), which are generated when over-expressed, and aberrant or tumor-associated autologous antigens (TAAs), which are captured by immune cells, have been considered to be effective in the early detection of lung cancer.^{10,11} Unexpectedly, some studies pointed out that positive results of AABs can be detected even before the formation of visible lesions on CT scans.^{12,13} A previous study on the diagnostic value of 10 AABs (p53, NY-ESO-1, Survivin, c-myc, cyclin B1, GBU4-5, CAGE, P16, SOX2, and HuD) found that each AAB on its own showed excellent specificity but poor sensitivity.¹⁴ A test that detected the presence of seven AABs (p53, NY-ESO-1, GBU4-5, CAGE, SOX2, HuD, and MAGE A4) in a panel using an indirect enzyme-linked immunosorbent assay (ELISA) performed in approximately 1600 European patients showed 87% specificity, 41% sensitivity and a 5.4-fold relative risk of lung cancer in patients with a positive test result.¹⁵ Detection using a panel of seven AABs (p53, GAGE7, PGP9.5, CAGE, MAGEA1, SOX2 and GB14-5) selected specifically

for the Chinese population was approved by the China Food and Drug Administration (CFDA) for assisting in diagnosing lung cancer.¹⁶ However, to our knowledge, there have been no studies comparing the diagnostic value of the 7-AAB panel with CT diagnosis in the same population, especially for patients whose preliminary radiological diagnosis is undetermined; in addition, no study has combined the 7-AAB result with radiologic and clinical characteristics to achieve a higher diagnostic accuracy.

In this study, we prospectively evaluated the diagnostic value of the 7-AAB panel and compared it with that of CT diagnosis in the same population with different stages, imaging features, pathological types, and diameters. In addition, we constructed a nomogram and formulated a scoring table including the 7-AAB panel results and radiologic and clinical characteristics to assist in distinguishing benign nodules from malignancy, which is useful in clinical application.

2 | MATERIALS AND METHODS

2.1 | Patients and grouping

The study was approved by the Medical Ethics Committee and institutional review board of The First Affiliated Hospital, Zhejiang University.

This study initially included 365 patients who presented with radiological ground-glass opacities (GGOs) and/or solid nodules and underwent both the 7-AAB panel test and pathological diagnosis at The First Affiliated Hospital, Zhejiang University between June 2018 and August 2019. The diagnostic procedure is shown in Figure 1A. The CT diagnoses were reported by at least two experienced radiologists. Patients whose preliminary radiological diagnosis was undetermined or recommended for follow-up were rediagnosed by another more experienced radiologist. The eligibility criteria were as follows: (a) patients were diagnosed with pulmonary GGOs and/or nodules by CT; (b) patients were diagnosed with NSCLC or benign disease pathologically after surgical resection according to the World Health Organization (WHO) classification;¹⁷ and (c) patients who were diagnosed with NSCLC could be staged according to the 8th edition of the American Joint Committee on Cancer lung cancer staging classification.¹⁸ The exclusion criteria were as follows: (a) patients with a pathological diagnosis by bronchoscope biopsy or needle biopsy; (b) patients who suffered other malignancies; (c) patients with more than one lesion considered malignant by multi-disciplinary team, but not all lesions were resected, and the pathological result was benign; (d) patients with invalid 7-AAB test results; (e) patients who underwent antitumor therapy before; and (f) patients with incomplete clinicopathological data (Figure 1B).

Finally, 268 patients were included for further investigation. All these patients were randomly assigned a number using a table of random numbers. The patients numbered 1 to 100 were allocated to the training group while the others were allocated to the validation group.

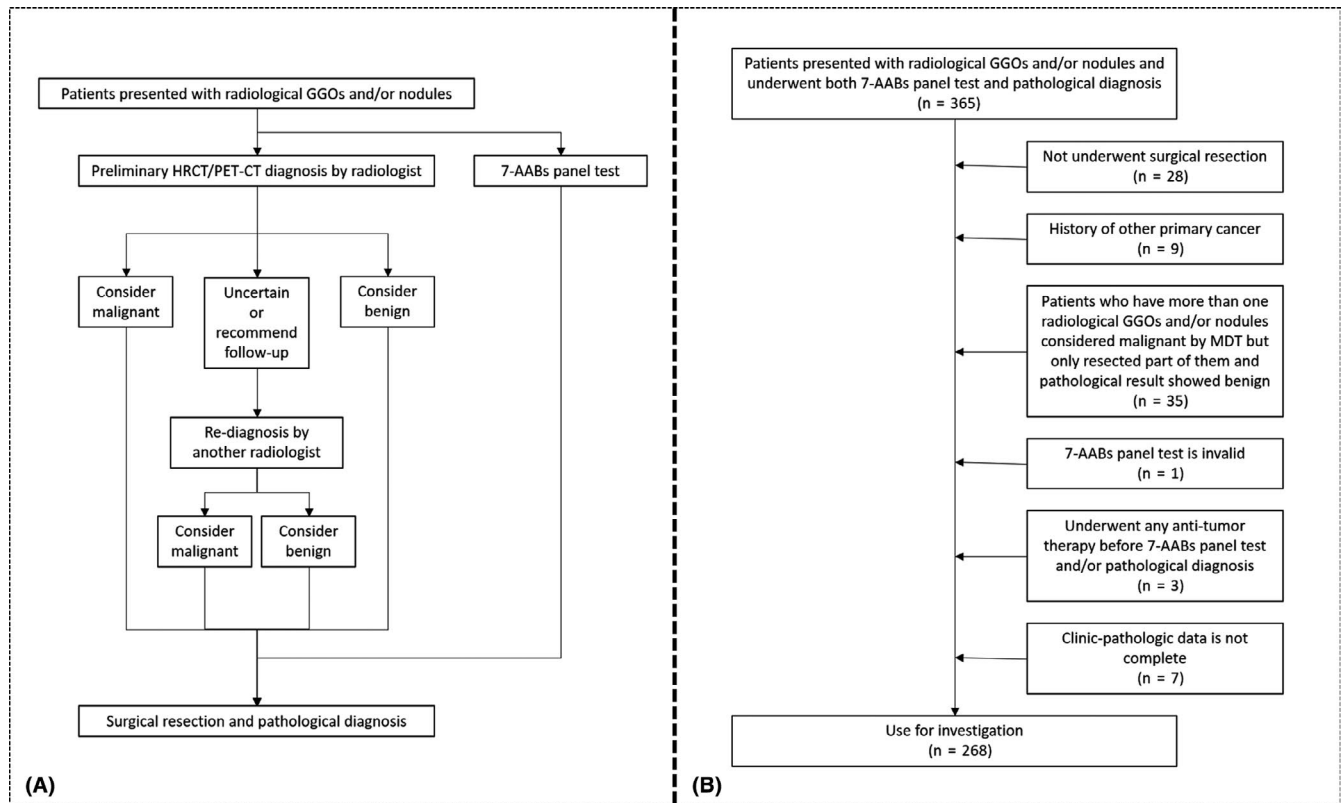


FIGURE 1 Flowchart of this study. A, Diagnostic procedure. B, Inclusion and exclusion criteria. AABs, autoantibodies; GGO, ground-glass opacity; HRCT, high-resolution computed tomography; PET-CT, positron emission tomography-computed tomography

2.2 | Quantitative and qualitative features of the autoantibodies

A detection kit of seven different AABs (Cancer Probe Biological Technology Co., Ltd., Hangzhou, China) was used according to the manufacturer's recommendations. In brief, 1 ng of anti-Myc IgG was added to 1 mL PBS as a standard control, and the optical density (OD) of the above-mentioned solution at 450 nm was read using a spectrophotometer. This OD value was defined as 1 u/mL. Serum samples and detection kit components were equilibrated to room temperature and diluted based on the instructions. Antigen-coated wells were washed with 200–300 μ L of 1 \times PBS for 1 min. Then, 50 μ L of diluted serum samples, standards, and controls were added to the antigen-coated wells and wells were incubated at room temperature for 1 h. Plates were washed three times using a Microplate Washer and following the standard procedure, next 50 μ L of diluted secondary antibodies against human IgG HRP was added and the plates incubated for 30 min. Thereafter, the plates were once again washed three times as above, and then 100 μ L of substrate were added, followed by plate incubation for 15 min at room temperature. Subsequently, 50 μ L of stop solution was added to each well and mixed thoroughly. The OD at 450 nm was read within 30 min using a spectrophotometer.

The cutoffs for p53, PGP9.5, SOX2, GACE7, GBU4-5, MAGEA1, and CAGE were 13.1, 11.1, 10.3, 14.4, 7.0, 11.9, and 7.2 u/mL, respectively.¹⁶ The result was considered positive if at least one AAB was elevated above the cutoff.

2.3 | Statistical analysis

Categorical variables were calculated using the chi-squared (χ^2) test and Fisher exact test, while continuous variables were analyzed using t test. The sensitivity and specificity were compared by matching χ^2 tests. The area under the curve (AUC) and its standard error (SE) for the receiver operating characteristic (ROC) curves were used to evaluate the diagnostic value. Logistic regression was used to compare the respective AUCs and construct the nomogram. The performance of the nomogram was assessed by discrimination and calibration. For all the analyses, two-sided *P*-values of <.05 were considered statistically significant. All analyses were performed using SPSS 22.0 software (IBM, Armonk, NY), GraphPad Prism 7.0 software (GraphPad software, La Jolla, CA), Med-Calc 19.1 (Med-Calc software, Ostend, Belgium) and R 3.6.1 (The R Foundation for Statistical Computing, Vienna, Austria) with the rms statistical package.

3 | RESULTS

3.1 | Study population

To investigate the diagnostic efficiency of the 7-AAB panel, 268 patients were enrolled in our study. The major clinicopathological characteristics of the patients in this study are summarized

in Table 1. The study included 207 patients with NSCLC and 61 patients with benign lung disease. Most of these patients had imaging features as pure GGO with a diameter less than or equal to 2 cm. For those who had malignant disease, 92.3% were patients with stage I disease.

3.2 | The concentration and diagnostic efficiency of the 7-AAB panel compared with CT scanning in the full cohort

Our results showed that the serum concentrations of all seven AABs in patients with NSCLC were higher than those in patients with benign disease, and the differences in SOX2, GBU4-5, MAGEA1, and GAGE values were statistically significant ($P < .001$, $P = .002$, $P = .007$, and $P = .003$, respectively) (Table 2). Almost all seven AABs, except p53 and PGP9.5, presented a discrimination between malignant and benign disease in qualitative diagnosis.

Combining all seven AABs, the reactivity of the AABs panel and CT diagnosis in patients with malignant disease or benign disease is shown in Table S1. The sensitivity, specificity, and positive predictive values (PPV) compared with CT were 36.7% vs 57.5% ($P < .001$), 90.2% vs 32.8% ($P < .001$), and 92.7% vs 74.4% ($P = .001$), respectively (Figure 2A). We also conducted subgroup analyses to explore the diagnostic efficiency of the 7-AAB panel in patients with different pathological types, imaging features, diameters, and stages compared with CT diagnosis. Interestingly, for patients with pure GGOs, the specificity and PPV results from the 7-AAB panel were much higher than those found by CT scanning (90.9% vs 27.3% [$P < .001$]; and 93.2% vs 71.4% [$P = .001$], respectively). A similar trend was also observed in lesions with diameters <1 cm or between 1 and 2 cm (Table S2). When we compared the sensitivity in noninvasive adenocarcinomas such as MIA or AIS for CT diagnosis, the 7-AAB panel demonstrated a higher sensitivity (41.5% vs 17.1% [$P = .001$]). The detailed results are shown in Figure 2B–J and Table S2.

3.3 | The concentration and diagnostic efficiency of the 7-AAB panel compared with CT in the preliminary undetermined radiological diagnosis group

Another experienced radiologist was asked to perform the rediagnosis for those patients whose preliminary radiological diagnoses were undetermined or recommended for follow-up. The baseline characteristics are shown in Table 1. Compared with the full cohort, the diameter of the nodules was smaller, and the proportion of GGOs and patients with early-stage disease (especially MIA or AIS) was higher in this group.

SOX2, MAGEA1 and GAGE concentrations were higher in patients with malignant disease ($P = .020$, $P = .037$, and $P = .040$, respectively) (Table 2). A similar comparison was also conducted between the 7-AAB panel and CT diagnosis. The results demonstrated that the

sensitivity, specificity, and PPV of the 7-AAB panel were higher than those of CT diagnosis (30.8% vs 19.2% [$P = .038$]; 87.5% vs 31.2% [$P < .001$]; and 80.0% vs 31.2% [$P = .001$]), respectively (Figure 3A; Table S2). Moreover, in patients with noninvasive adenocarcinoma, a similar trend was also observed: the sensitivity and PPV of the 7-AAB panel were higher than those of CT diagnosis (29.4% vs 11.8% [$P = .006$]; 100.0% vs 33.3% [$P = .045$]) (Figure 3B; Table S2).

3.4 | Predictive nomogram for the probability of malignant disease when combining the 7-AAB panel with other clinical characteristics

For further investigation, a nomogram was constructed that incorporated the 7-AAB panel and six other risk factors for predicting malignant disease (Figure 4A). A total score was calculated with the use of the 7-AAB panel, CT diagnosis, composition of nodules, diameters of nodules, numbers of nodules, sex, and age. The score of each factor is shown on the point calibration axis. The total points were calculated by adding the scores of each factor to estimate the possibility of malignant disease. A calibration curve of the nomogram is shown in Figure 4B, which demonstrates that the malignant disease probabilities predicted by the nomogram accorded well with the actual probability.

3.5 | A handy scoring table based on the 7-AAB panel combined with other clinical characteristics

For more convenient use in clinical diagnosis, we constructed a scoring table (Table 3) in the training group based on the nomogram that combined the 7-AAB panel and other clinical characteristics (including some factors not included in the nomogram but we believed were useful in clinical diagnosis), and then we evaluated its diagnostic efficiency in the validation group. The baseline of the two groups was similar except that there were more undetermined preliminary radiological diagnosis patients in the validation group (Table 4).

The score was significantly correlated with the diagnosis of malignant disease in the training group. The sensitivity and specificity using the cutoff value of 9.75 were 75.64% and 81.82%, respectively. The AUC was 0.840 (95% confidence interval [CI], 0.753–0.905) (Figure 5A), which was higher than the values found using the 7-AAB panel or CT alone (0.840 vs 0.589 [$P < .001$]; 0.840 vs 0.578 [$P = .003$]); (Figure 5B). Similar to the training group, using the cutoff of 9.75 in the validation group and drawing a ROC curve, the sensitivity and specificity were 86.05% and 69.23%, respectively (Figure 5C). Compared with using the 7-AAB panel and CT alone, the AUC was also higher (0.860 vs 0.660 [$P < .001$]; 0.860 vs 0.531 [$P < .001$]) (Figure 5D).

For patients whose preliminary radiological diagnosis was undetermined, the score also showed a good diagnostic value. The AUC was 0.774 (95% CI, 0.670–0.858; $P < .001$) (Figure 5E). In

TABLE 1 Clinicopathologic characteristics of the study population

Characteristics	Full cohort (n = 268)			Preliminary radiological diagnosis uncertain group (n = 84)		
	Patients with malignant disease (n = 207)	Patients with benign disease (n = 61)	P-value	Patients with malignant disease (n = 52)	Patients with benign disease (n = 32)	P-value
Age, y, mean (SD)	58.04 (11.50)	53.66 (10.42)	.008	53.69 (13.21)	52.81 (11.47)	.756
Gender, n (%)						
Male	94 (35.1)	30 (11.2)	.662	16 (19.0)	12 (14.3)	.635
Female	113 (42.2)	31 (11.5)		36 (42.9)	20 (23.8)	
Diameter, cm, mean (SD)	1.62 (1.08)	1.35 (1.62)	.131	1.30 (0.85)	0.93 (0.47)	.023
Group of diameters, n (%)						
$\varphi \leq 1$ cm	81 (30.2)	30 (11.2)	.026	31 (36.9)	21 (25.0)	.254
$1 \text{ cm} < \varphi \leq 2$ cm	78 (29.1)	25 (9.3)		12 (14.3)	10 (11.9)	
$2 \text{ cm} < \varphi \leq 3$ cm	28 (10.4)	4 (1.5)		7 (8.3)	1 (1.2)	
$\varphi > 3$ cm	20 (7.5)	2 (0.8)		2 (2.4)	0 (0.0)	
Number of nodules, n (%)						
Single	111 (41.4)	40 (14.9)	.108	22 (26.2)	18 (21.4)	.263
Multiple	96 (35.8)	21 (7.9)		30 (35.7)	14 (16.7)	
Composition, n (%)						
Pure GGO	162 (60.4)	44 (16.4)	.169	44 (52.4)	27 (32.0)	.163
Mix GGO	10 (3.7)	1 (0.4)		4 (4.8)	0 (0.0)	
Solid nodule	35 (13.1)	16 (6.0)		4 (4.8)	5 (6.0)	
Pathologic type, n (%)						
Adenocarcinoma	152 (56.7)	0		34 (40.5)	0	
SCC	12 (4.5)	0		1 (1.2)	0	
AIS or MIA	41 (15.3)	0		17 (20.2)	0	
Neuroendocrine neoplasm	2 (0.7)	0		0	0	
Lung benign tumor	0	9 (3.4)		0	3 (3.6)	
Nontumor benign disease	0	41 (15.3)		0	22 (26.2)	
AAH	0	11 (4.1)		0	7 (8.3)	
Stage, n (%)						
I	191 (92.3)	0		50 (96.2)	0	
II	5 (2.4)	0		1 (1.9)	0	
III	10 (4.8)	0		1 (1.9)	0	
IV	1 (0.5)	0		0 (0.0)	0	
Speculation sign, n (%)	150 (72.5)	28 (45.9)	<.001	31 (59.6)	11 (34.4)	.042
Pleural indentation, n (%)	45 (21.7)	5 (1.9)	.015	9 (17.3)	2 (6.2)	.193
Vessels sign, n (%)	80 (38.6)	9 (14.8)	<.001	19 (36.5)	4 (12.5)	.023
Air bronchogram, n (%)	34 (16.4)	4 (6.6)	.035	9 (17.3)	1 (3.1)	.081

patients with AIS or MIA, the score can also provide an accurate prediction, and the AUC was 0.742 (95% CI, 0.646-0.823; $P < .001$) (Figure 5F).

Overall, 170 (91.4%) of 186 patients with high scores and 37 (45.1%) of 82 patients with low scores suffered malignant disease, and the difference was statistically significant ($P < .001$). This trend

TABLE 2 Concentration and reactivity of each autoantibody (AAB)

	Full cohort (n = 268)			Preliminary radiological diagnosis uncertain group (n = 84)		
	Patients with malignant disease (n = 207)	Patients with benign disease (n = 61)	P-value	Patients with malignant disease (n = 52)	Patients with benign disease (n = 32)	P-value
p53 concentration, u/mL, (SD)	3.67 (6.37)	3.11 (5.55)	.535	5.00 (8.71)	3.13 (5.94)	.287
p53 qualitative diagnosis, n (%)						
Positive	17 (6.3)	4 (1.5)	.672	5 (6.0)	3 (3.5)	.971
Negative	190 (70.9)	57 (21.3)		47 (56.0)	29 (34.5)	
PGP9.5 concentration, u/mL, (SD)	1.90 (7.68)	1.87 (7.86)	.976	2.38 (11.05)	3.16 (10.73)	.749
PGP9.5 qualitative diagnosis, n (%)						
Positive	6 (2.2)	2 (0.8)	.878	1 (1.2)	2 (2.4)	.308
Negative	201 (75.0)	59 (22.0)		51 (60.7)	30 (35.7)	
SOX2 concentration, u/mL, (SD)	4.45 (7.62)	2.11 (2.68)	<.001	5.28 (8.95)	2.16 (2.41)	.020
SOX2 qualitative diagnosis, n (%)						
Positive	25 (9.3)	1 (0.4)	.015	6 (7.1)	0 (0.0)	.014
Negative	182 (67.9)	60 (22.4)		46 (54.8)	32 (38.1)	
GACE7 concentration, u/mL, (SD)	4.55 (7.27)	3.43 (5.84)	.215	4.87 (6.16)	3.86 (7.70)	.511
GACE7 qualitative diagnosis, n (%)						
Positive	16 (6.0)	1 (0.4)	.051	4 (4.8)	1 (1.2)	.369
Negative	191 (71.2)	60 (22.4)		48 (57.1)	31 (36.9)	
GBU4-5 concentration, u/mL, (SD)	2.56 (3.67)	1.48 (1.79)	.002	1.60 (2.27)	1.70 (2.13)	.831
GBU4-5 qualitative diagnosis, n (%)						
Positive	26 (9.7)	1 (0.4)	.013	2 (2.4)	1 (1.2)	.862
Negative	181 (67.5)	60 (22.4)		50 (59.5)	31 (36.9)	
MAGEA1 concentration, u/mL, (SD)	1.55 (4.48)	0.50 (1.74)	.007	3.02 (7.22)	0.70 (2.38)	.037
MAGEA1 qualitative diagnosis, n (%)						
Positive	8 (3.0)	0 (0.0)	.040	5 (6.0)	0 (0.0)	.026
Negative	199 (74.2)	61 (22.8)		47 (56.0)	32 (38.0)	
GAGE concentration, u/mL, (SD)	1.39 (4.87)	0.32 (0.76)	.003	2.48 (7.43)	0.30 (0.43)	.040
GAGE qualitative diagnosis, n (%)						
Positive	12 (4.5)	0 (0.0)	.012	6 (7.1)	0 (0.0)	.014
Negative	195 (72.8)	61 (22.7)		46 (54.8)	32 (38.1)	

still existed for those whose preliminary radiological diagnosis was undetermined. We also analyzed the relationship between the score and other clinicopathological characteristics, and the results are summarized in Table 5.

4 | DISCUSSION

The clinical utility of the 7-AAB panel in the Chinese population has not been fully validated compared with CT diagnosis, and the combination of the 7-AAB panel with clinical-radiologic characteristics in the early detection of NSCLC remains challenging. In our study, we validated the diagnostic value of a panel of seven AABs in patients

presenting with lesions on CT screening and then compared its diagnostic value with CT diagnosis. Our results indicated that the 7-AAB panel had significant value in diagnosing NSCLC. Subsequently, we developed a nomogram containing the 7-AAB panel test result and other clinical-radiologic characteristics that can predict the risk of malignancy for patients with a lesion on CT screening. For convenient clinical application, we additionally constructed a scoring table based on the nomogram, and validation by the ROC curves indicated that the scoring table has clinical utility even for patients with noninvasive lung cancer or those whose preliminary radiological diagnosis was undetermined.

LDCT has been widely used in lung cancer screening, and an increasing number of nodules, especially pure GGOs and mixed GGOs,

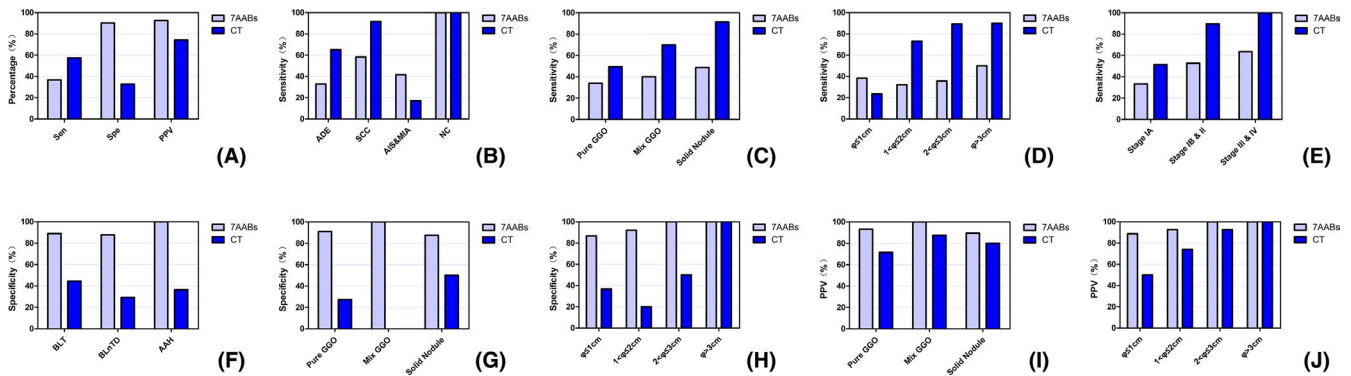


FIGURE 2 Diagnostic performance of the 7-AAB panel compared with that of CT. A, Diagnostic value in the full cohort. B, Subanalysis of sensitivity according to pathological type. C, Subanalysis of sensitivity according to solid proportion. D, Subanalysis of sensitivity according to diameter. E, Subanalysis of sensitivity according to pathological stage. F, Subanalysis of specificity according to pathological type. G, Subanalysis of specificity according to solid proportion. H, Subanalysis of specificity according to diameter. I, Subanalysis of PPV according to solid proportion. J, Subanalysis of PPV according to diameter

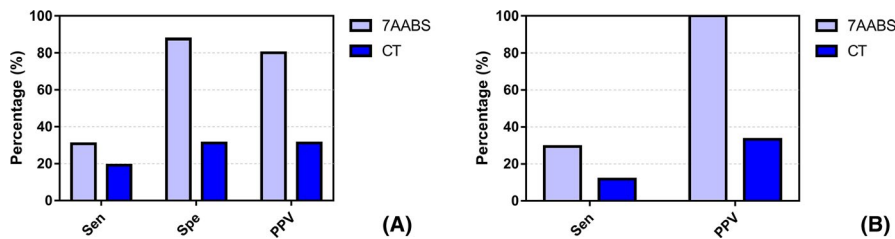


FIGURE 3 Diagnostic performance of the 7-AAB panel compared with that of CT in patients whose preliminary radiological diagnosis was undetermined. A, Sensitivity, specificity, and PPV of the 7-AAB panel in patients whose preliminary radiological diagnosis was undetermined. B, Specificity and PPV of the 7-AAB panel in patients with noninvasive pathological types whose preliminary radiological diagnosis was undetermined

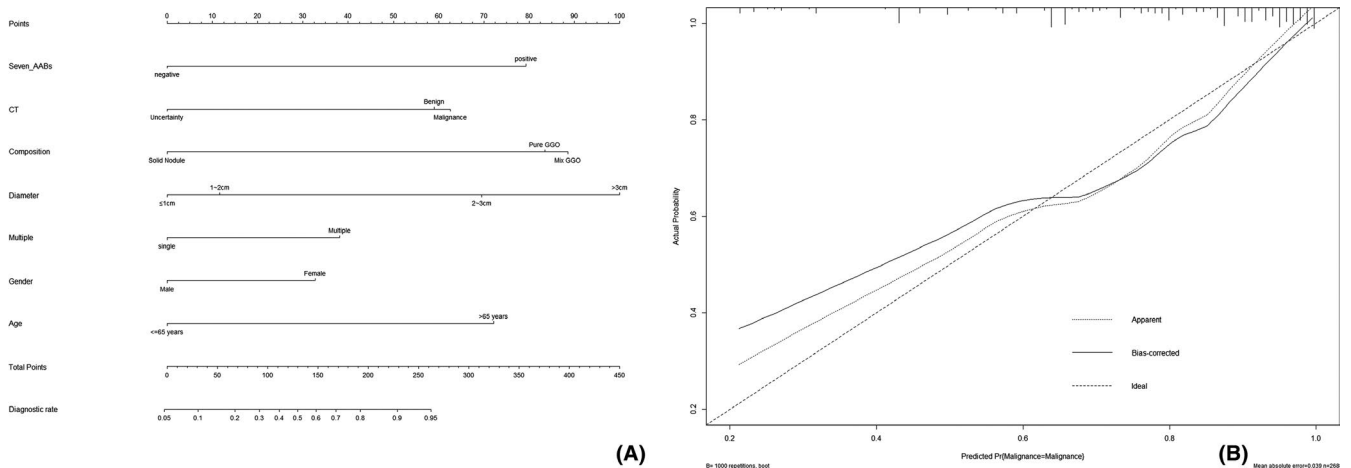


FIGURE 4 A nomogram predicting the risk of non-small-cell lung cancer. A, A nomogram predicting the probability of non-small-cell lung cancer. The value of each factor was given a score on the point scale axis. A total score could be calculated by adding every single score together and by projecting the total score to the total point scale so that clinicians can estimate the probability of NSCLC. B, The calibration curves for the nomogram. The x-axis represents the probability predicted by the nomogram, and the y-axis represents the actual probability of NSCLC

have been detected. However, it is difficult for LDCT to distinguish early-stage lung cancer from benign disease, subsequently leading to a high false-positive rate that causes excessive medical intervention with unnecessary psychological burden to patients.¹⁹ In addition,

the value of LDCT in reducing mortality has also been questioned.²⁰ Furthermore, for patients with pure GGOs less than 2 cm, the pathological types are often AIS or MIA, which only need sublobar resection, and the 5-y survival rate is approximately 100%. As the imaging

TABLE 3 Scoring table for predicting the risk of non-small-cell lung cancer

Index	Status	Score
7AABs	Negative	0
	Positive	5
Preliminary radiological diagnosis	Uncertain	0
	Benign	2.5
	Malignant	3
Diameter	$\varphi \leq 1$ cm	0
	$1 \text{ cm} < \varphi \leq 2$ cm	1
	$2 \text{ cm} < \varphi \leq 3$ cm	3.5
	$\varphi > 3$ cm	4.5
Number of nodules	Single	0
	Multiple	2
Gender	Male	0
	Female	1.5
Age	<65 y	0
	≥ 65 y	3.5
Speculation sign	Negative	0
	Positive	2
Pleural indentation	Negative	0
	Positive	1
Vessels sign	Negative	0
	Positive	2
Air bronchogram	Negative	0
	Positive	1

features of these patients are often nontypical and need long-term follow-up, the disease can develop to a more advanced stage with a worse prognosis. Therefore, it is essential to formulate a novel test in the early diagnosis of lung cancer, especially for patients with non-invasive disease that can assist in the evaluation of the malignancy of pulmonary nodules in the clinic. Liquid biopsy shows potential in this aspect for its superiorities such as being noninvasive, objectively accessible, and easily repeated. To date, various biomarkers such as TAAs, microRNAs, circulating tumor cells (CTCs), and tumor-associated autoantibody panels have been used to adjunctively diagnose lung cancer.²¹⁻²⁵

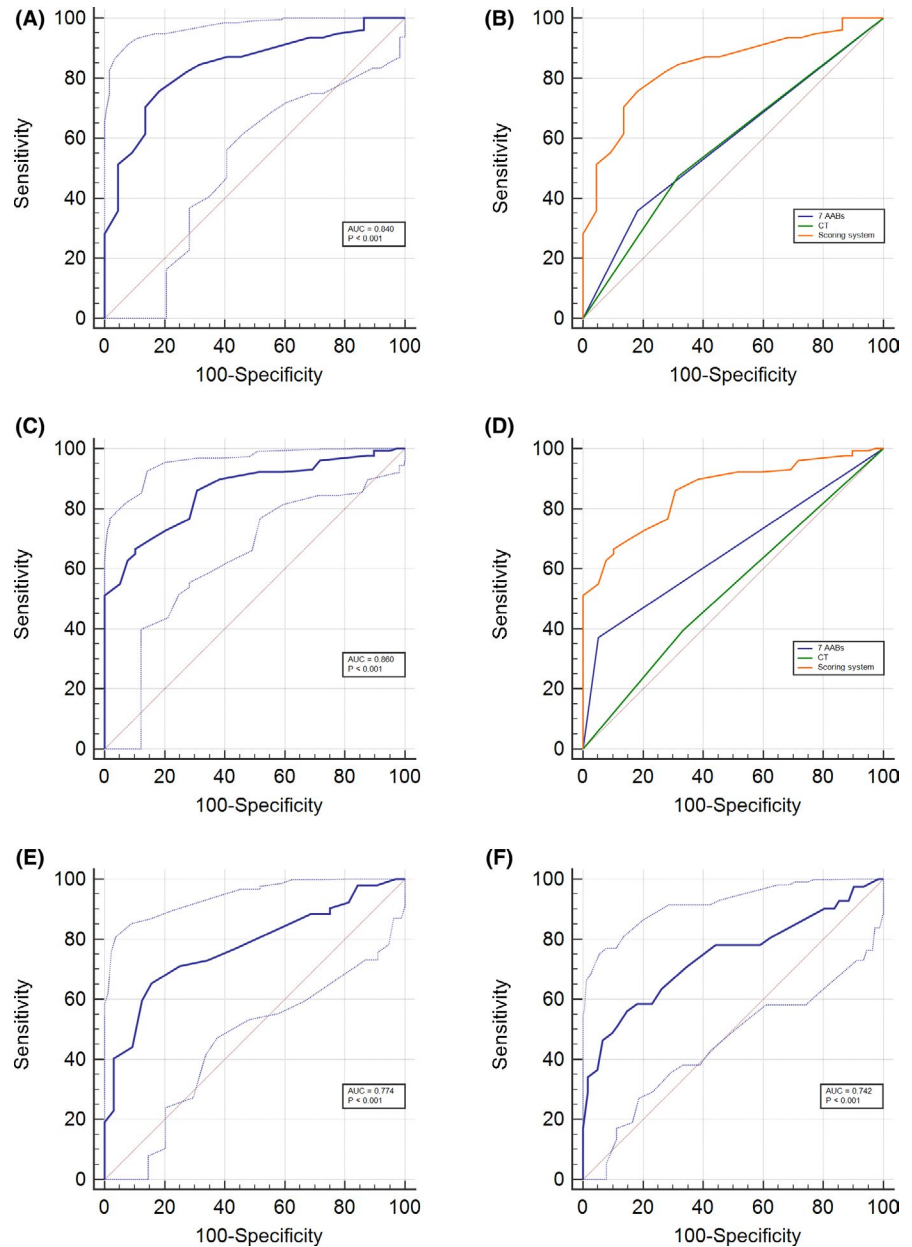
Among these, studies have discovered AABs associated with lung cancer that have the potential to distinguish malignant disease from CT-positive benign nodules.²⁶ In Europe, EarlyCDT-Lung, which contains a panel of seven AABs (p53, NY-ESO-1, GBU4-5, CAGE, SOX2, HuD, and MAGE A4), was confirmed to have 87% specificity and 41% sensitivity.^{15,27} Additionally, a positive EarlyCDT-Lung panel result was associated with a 5.4-fold increase in lung cancer incidence versus a negative result.²⁸ Because of the large differences in the genetic makeup between European and Asian populations, a similar study was performed in Chinese patients using the 7-AAB panel, which was specially selected for the Chinese population. Under the optimal cutoff value for each

TABLE 4 Demographics and clinicopathologic characteristics of the training group and validation group

	Training group (n = 100)	Validation group (n = 168)	P-value
Age, y, mean (SD)	55.55 (11.40)	57.93 (11.34)	.099
Gender, n (%)			
Male	43 (43.0)	81 (48.2)	.448
Female	57 (57.0)	87 (51.8)	
Diameter, cm, mean (SD)	1.37 (0.83)	1.67 (1.40)	.055
Number of nodules, n (%)			
Single	54 (54.0)	97 (57.7)	.551
Multiple	46 (46.0)	71 (42.3)	
Composition, n (%)			
Pure GGO	74 (74.0)	132 (78.6)	.439
Mix GGO	6 (6.0)	5 (3.0)	
Solid nodule	20 (20.0)	31 (18.4)	
Pathologic type, n (%)			
Adenocarcinoma	59 (59.0)	93 (55.3)	.447
SCC	2 (2.0)	10 (6.0)	
AIS or MIA	17 (17.0)	24 (14.3)	
Neuroendocrine neoplasm	0 (0.0)	2 (1.2)	
Lung benign tumor	4 (4.0)	5 (3.0)	
Nontumor benign disease	16 (16.0)	25 (14.9)	
AAH	2 (2.0)	9 (5.3)	
Stage, n (%)			
I	73 (93.6)	118 (91.5)	.743
II	2 (2.6)	3 (2.3)	
III	3 (3.8)	7 (5.4)	
IV	0 (0.0)	1 (0.8)	
Speculation sign, n (%)	57 (57.0)	121 (72.0)	.016
Pleural indentation, n (%)	19 (19.0)	31 (18.5)	.911
Vessels sign, n (%)	39 (39.0)	50 (29.8)	.120
Air bronchogram, n (%)	14 (14.0)	24 (14.3)	.948
Preliminary radiological diagnosis			
Benign	13 (13.0)	43 (25.6)	.014
Malignant	47 (47.0)	81 (48.2)	
Uncertain	40 (40.0)	44 (26.2)	
7-AABs qualitative diagnosis			
Positive	32 (32.0)	50 (29.8)	.701
Negative	68 (68.0)	118 (70.2)	

AAB, the sensitivity and specificity were 61% and 90%, respectively, which were higher than those of traditional biomarkers.¹⁶ Another study also demonstrated that using a combination of 22

FIGURE 5 ROC curve using the scoring table to predict NSCLC. A, ROC curve using the scoring table to predict NSCLC in the training group. B, ROC curve using the scoring table to predict NSCLC in the training group compared with using the 7-AAB panel or CT alone. C, ROC curve using the scoring table to predict NSCLC in the validation group. D, ROC curve using the scoring table to predict NSCLC in the validation group compared with using the 7-AAB panel or CT alone. E, ROC curve using the scoring table to predict NSCLC in patients whose preliminary radiological diagnosis was undetermined. F, ROC curve using the scoring table to predict NSCLC in patients whose pathological type was AIS or MIA. In graph A, C, E, F respectively, the blue solid line is the exact ROC curve, and the blue dotted line is the 95% CI of this ROC curve. And the red dotted line is the line of reference whose AUC is 0.500



autoantibody biomarkers could detect preneoplastic lung lesions.²⁹ Our data are consistent with these findings. In this study, our 7-AAB panel achieved a specificity of over 90% and a PPV of over 92%, which were significantly higher compared with those of CT diagnosis. Interestingly, for patients with noninvasive malignancy or whose preliminary radiological diagnosis was undetermined, the diagnostic value of the seven AABs showed greater superiority compared with CT, even in sensitivity.

Unlike Ren et al's study, the sensitivity observed in our study, which is similar to that of the EarlyCDT-Lung test, was not as high, even when we used the same panel of AABs. However, the PPV of our study was higher than that of the previous study. This result is probably due to the following reasons:

(a) First, the cutoff value of the 7-AAB panel we used was determined by Ren et al's study in 155 patients with lung cancer and in 145 healthy controls. Although this cutoff value was optimal

for their study population, it may not be repeatable in other study populations with the same diagnostic value even though the ethnic groups were the same.

(b) Second, a previous study reported that the levels of autoantibodies were increased in the advanced stage.³⁰ In our study, more than 85% of our patients had stage IA disease, and among these, nearly one-quarter had noninvasive malignancies, such as AIS or MIA. Thus, the concentration of those patients' AABs may not as high as that of advanced patients to reach the cutoff value and show a positive result.

(c) Third, most of the patients enrolled in our study had a radiographic feature of GGOs with a diameter less than 2 cm, which are often noncalcified. These patients are recommended to receive anti-inflammatory therapy and follow-up.

A recent study pointed out that antibiotic treatment is associated with a worse immune response,³¹ which may also be a potential

TABLE 5 Relationship between the score and clinicopathologic characteristics

Characteristics	Full cohort (n = 268)			Preliminary radiological diagnosis uncertain group (n = 84)		
	Low score group (n = 82)	High score group (n = 186)	P-value	Low score group (n = 49)	High score group (n = 35)	P-value
Pathological diagnosis						
Benign	45 (54.9)	16 (8.6)	<.001	28 (57.1)	4 (11.4)	<.001
Malignant	37 (45.1)	170 (91.4)		21 (42.9)	31 (88.6)	
Age, y, mean (SD)	50.98 (9.84)	59.72 (11.02)	<.001	50.35 (9.47)	57.57 (14.98)	.008
Gender, n (%)						
Male	36 (43.9)	88 (47.3)	.606	16 (32.7)	12 (34.3)	.876
Female	46 (56.1)	98 (52.7)		33 (67.3)	23 (65.7)	
Diameter, cm, mean (SD)	1.17 (1.40)	1.73 (1.11)	.002	0.91 (0.43)	1.51 (0.94)	<.001
Number of nodules, n (%)						
Single	53 (64.6)	98 (52.7)	.069	26 (53.1)	14 (40.0)	.237
Multiple	29 (35.4)	88 (47.3)		23 (46.9)	21 (60.0)	
Composition, n (%)						
Pure GGO	63 (76.8)	143 (76.9)	.232	43 (87.8)	28 (80.0)	.025
Mix GGO	1 (1.2)	10 (5.4)		0 (0.0)	4 (11.4)	
Solid nodule	18 (22.0)	33 (17.7)		6 (12.2)	3 (8.6)	
Pathologic type, n (%)						
Adenocarcinoma	21 (25.6)	131 (70.4)	<.001	11 (22.4)	23 (65.7)	<.001
SCC	1 (1.2)	11 (5.9)		0 (0.0)	1 (2.9)	
AIS or MIA	15 (18.3)	26 (14.0)		10 (20.4)	7 (20.0)	
Neuroendocrine neoplasm	0 (0.0)	2 (1.1)		0 (0.0)	0 (0.0)	
Lung benign tumor	6 (7.3)	3 (1.6)		2 (4.1)	1 (2.9)	
Nontumor benign disease	29 (35.4)	12 (6.5)		19 (38.8)	3 (8.5)	
AAH	10 (12.2)	1 (0.5)		7 (14.3)	0 (0.0)	
Stage, n (%)						
I	37 (100.0)	154 (90.6)	.066	21 (100.0)	29 (93.6)	.346
II	0 (0.0)	5 (2.9)		0 (0.0)	1 (3.2)	
III	0 (0.0)	10 (5.9)		0 (0.0)	1 (3.2)	
IV	0 (0.0)	1 (0.6)		0 (0.0)	0 (0.0)	
Preliminary radiological diagnosis, n (%)						
Benign	19 (23.1)	37 (19.9)	<.001	/	/	/
Malignant	14 (17.1)	114 (61.3)		/	/	
Uncertain	49 (59.8)	35 (18.8)		/	/	
7-AABs qualitative diagnosis, n (%)						
Positive	3 (3.7)	79 (42.5)	<.001	3 (6.1)	17 (48.6)	<.001
Negative	79 (96.3)	107 (57.5)		46 (93.9)	18 (51.4)	

reason for our study's sensitivity. Even so, the sensitivity of our seven AAB panel was as high as that of the EarlyCDT-Lung test and significantly higher than that of traditional tumor markers.^{27,32} Surprisingly, for patients with noninvasive NSCLC or those whose preliminary radiological diagnosis was undetermined, the sensitivity of our 7-AAB panel was much higher than that of CT diagnosis.

Because of the diagnostic value of our 7-AAB panel, we created a nomogram based on the 7-AAB test results to quantify the risk of NSCLC. In addition to the 7-AAB results, the predictive model also contained preliminary CT diagnosis, composition of nodules, diameter of nodules, number of lesions, sex, and age. The previous study only combined the seven AABs with CT imaging using a simple

both-positive rule to increase the PPV, but the change was not visible compared with using the 7-AAB test alone, and it reduced the sensitivity at the same time.¹⁶ In spite of this 7-AAB panel being reported previously, our study is the first prospective study conducted in Zhejiang province's population, who have not been validated before, and after this 7-AAB panel was approved by CFDA. Although the sensitivity of our 7-AAB panel was not as high as CT diagnosis, our 7-AAB panel was of a very high PPV. Such a high PPV may indicated that clinicians could perform surgical intervention more actively if the test showed a positive result and could avoid unnecessary follow-up. Contrary to the previous studies, for validation of the diagnostic value of this panel, we mainly focused on very early-stage disease, which present GGOs with diameters less than 2 cm on CT, especially those whose preliminary radiological diagnosis was undetermined or whose pathologic type was AIS or MIA. Moreover, the emphasis of our study was on combining the high specificity and PPV of 7-AAB panel and the high sensitivity of CT diagnosis to conduct a visual statistical model that could optimize the predictive accuracy of each individual. To our knowledge, our study was the first to construct a quantitative nomogram that could predict the probability of NSCLC with optimal discrimination and excellent calibration. In our nomogram, the 7-AAB panel result contributes a great risk proportion of malignancy. In addition, we formulated a scoring table based on the nomogram for the purpose of more convenient application. This table can calculate the total points more easily and may support clinicians when making treatment decisions. In both the training group and validation group, using the scoring table resulted in optimal diagnostic accuracy, which was significantly higher than using CT or the 7-AAB panel alone. The widespread use of LDCT has increased the detection of pure or mixed GGOs with diameters less than 2 cm, a size that is hard for radiologists to diagnose.³³ Even for these patients, our scoring table can significantly enhance the diagnostic accuracy. Because of its high accuracy, this scoring table could help clinicians make appropriate therapeutic decisions, such as avoiding unnecessary operation or needless follow-up in patients with preneoplastic lung lesions.

Several limitations of this study should be addressed. First, we only enrolled patients who underwent surgical resection, and the sample size was not very large, especially for patients with benign disease; this choice may have caused selection bias. Second, although our predictive model and scoring table had been validated internally and showed excellent diagnostic value, the generalizability of the model and scoring table still needs external validation by an additional study population. The next step would be for us to investigate the diagnostic value of the 7-AAB panel in a prospective study that is controlled by a formal protocol with a larger sample size from multiple centers. In addition to further validating the diagnostic value of the current 7-AAB panel, we should also investigate that if it is necessary to modify the current cutoff value for different stages disease, particularly for very early-stage disease, in our future study. Furthermore, healthy donors who do not have any lung nodules should be included in the future study as a blank control. Wider geographic recruitment and additional data, such as CT value and positron emission tomography (PET) standardized uptake value

(SUV), could also be included in the model and scoring table, to improve the predictive accuracy for future applications.

In conclusion, we prospectively validated the diagnostic value of a 7-AAB panel in NSCLC that achieved a specificity of 90.2% and a PPV of 92.7%. In comparison with CT, it showed a higher diagnostic value, especially for patients with early-stage disease. In addition, our study was the first to develop and internally validate a novel nomogram based on the 7-AAB panel for predicting the risk of NSCLC. Moreover, based on the nomogram, we formulated a scoring table that is easy to use in the clinic and is highly accurate. This scoring table could help clinicians make individualized predictions of the probability of NSCLC and avoid over-management or reduce the period of needless follow-up. In summary, the 7-AAB panel test and our predictive model exhibited excellent potential for the diagnosis of NSCLC, and the scoring table could be of use to clinicians.

ACKNOWLEDGMENTS

This study was supported by Major Science and Technology Projects of Zhejiang Province (2014C03032), Key Disciplines of Traditional Chinese Medicine in Zhejiang Province (2017-XK-A33), National Key R&D Program of China (2017YFC0113500), and National Natural Science Foundation of China (31700690).

CONFLICT OF INTEREST

The authors have no conflicts of interest to declare.

ETHICAL APPROVAL

This study was approved by the Institute Research Medical Ethics Committee of The First Affiliated Hospital, School of Medicine, Zhejiang University, the reference number is 2018-536-2.

INFORMED CONSENT

All patients included in this research signed an informed consent according to the Research Ethics Committee of The First Affiliated Hospital, School of Medicine, Zhejiang University, China.

ORCID

Weidong Wang  <https://orcid.org/0000-0002-1168-8803>

Jian Hu  <https://orcid.org/0000-0002-9494-9828>

REFERENCES

1. Bray F, Ferlay J, Soerjomataram I, Siegel RL, Torre LA, Jemal A. Global cancer statistics 2018: GLOBOCAN estimates of incidence and mortality worldwide for 36 cancers in 185 countries. *CA Cancer J Clin*. 2018;68:394-424.
2. Miller KD, Siegel RL, Lin CC, et al. Cancer treatment and survivorship statistics, 2016. *CA Cancer J Clin*. 2016;66:271-289.
3. Chansky K, Detterbeck FC, Nicholson AG, et al. The IASLC Lung Cancer Staging Project: External Validation of the Revision of the TNM Stage Groupings in the Eighth Edition of the TNM Classification of Lung Cancer. *J Thorac Oncol*. 2017;12:1109-1121.
4. Henschke CI, Yankelevitz DF, Libby DM, Pasmantier MW, Smith JP, Miettinen OS. Survival of patients with stage I lung cancer detected on CT screening. *N Engl J Med*. 2006;355:1763-1771.

5. Aberle DR, DeMello S, Berg CD, et al. Results of the two incidence screenings in the National Lung Screening Trial. *N Engl J Med*. 2013;369:920-931.
6. Wood DE, Kazerooni EA, Baum SL, et al. Version 3.2018, NCCN Clinical Practice Guidelines in Oncology. *J Natl Compr Canc Netw*. 2018;16:412-441.
7. Horeweg N, Scholten ET, de Jong PA, et al. Detection of lung cancer through low-dose CT screening (NELSON): a prespecified analysis of screening test performance and interval cancers. *Lancet Oncol*. 2014;15:1342-1350.
8. Aberle DR, Adams AM, Berg CD, et al. Reduced lung-cancer mortality with low-dose computed tomographic screening. *N Engl J Med*. 2011;365:395-409.
9. Boiselle PM. Computed tomography screening for lung cancer. *JAMA*. 2013;309:1163-1170.
10. Mittal D, Gubin MM, Schreiber RD, Smyth MJ. New insights into cancer immunoediting and its three component phases—elimination, equilibrium and escape. *Curr Opin Immunol*. 2014;27:16-25.
11. Sullivan FM, Farmer E, Mair FS, et al. Detection in blood of autoantibodies to tumour antigens as a case-finding method in lung cancer using the EarlyCDT(R)-Lung Test (ECLS): study protocol for a randomized controlled trial. *BMC Cancer*. 2017;17:187.
12. Qiu J, Choi G, Li L, et al. Occurrence of autoantibodies to annexin I, 14-3-3 theta and LAMR1 in prediagnostic lung cancer sera. *J Clin Oncol*. 2008;26:5060-5066.
13. Boyle P, Chapman CJ, Holdenrieder S, et al. Clinical validation of an autoantibody test for lung cancer. *Ann Oncol*. 2011;22:383-389.
14. Qin J, Zeng N, Yang T, et al. Diagnostic value of autoantibodies in lung cancer: a systematic review and meta-analysis. *Cell Physiol Biochem*. 2018;51:2631-2646.
15. Chapman CJ, Healey GF, Murray A, et al. EarlyCDT(R)-Lung test: improved clinical utility through additional autoantibody assays. *Tumour Biol*. 2012;33:1319-1326.
16. Ren S, Zhang S, Jiang T, et al. Early detection of lung cancer by using an autoantibody panel in Chinese population. *Oncol Immunology*. 2017;7:e1384108.
17. Witt C. European respiratory society/american thoracic society/international association for the study of lung cancer international multidisciplinary classification of lung adenocarcinoma: state of the art. *J Thorac Oncol*. 2011;6:1451.
18. Detterbeck FC, Boffa DJ, Kim AW, Tanoue LT. The eighth edition lung cancer stage classification. *Chest*. 2017;151(1):193-203.
19. Croswell JM, Baker SG, Marcus PM, Clapp JD, Kramer BS. Cumulative incidence of false-positive test results in lung cancer screening: a randomized trial. *Ann Int Med*. 2010;152(505-512):w176-580.
20. Infante M, Cavuto S, Lutman FR, et al. Long-term follow-up results of the DANTE trial, a randomized study of lung cancer screening with spiral computed tomography. *Am J Respir Crit Care Med*. 2015;191:1166-1175.
21. Tarro G, Perna A, Esposito C. Early diagnosis of lung cancer by detection of tumor liberated protein. *J Cell Physiol*. 2005;203:1-5.
22. Chen X, Zhou F, Li X, et al. Folate receptor-positive circulating tumor cell detected by LT-PCR-based method as a diagnostic biomarker for non-small-cell lung cancer. *J Thorac Oncol*. 2015;10:1163-1171.
23. Liang W, Zhao Y, Huang W, Liang H, Zeng H, He J. Liquid biopsy for early stage lung cancer. *J Thorac Dis*. 2018;10:S876-S881.
24. Matikas A, Syrigos KN, Agelaki S. Circulating biomarkers in non-small-cell lung cancer: current status and future challenges. *Clin Lung Cancer*. 2016;17:507-516.
25. Solassol J, Maudelonde T, Mange A, Pujol JL. Clinical relevance of autoantibody detection in lung cancer. *J Thorac Oncol*. 2011;6:955-962.
26. Mazzone PJ, Sears CR, Arenberg DA, et al. Evaluating molecular biomarkers for the early detection of lung cancer: when is a biomarker ready for clinical use? An official american thoracic society policy statement. *Am J Respir Crit Care Med*. 2017;196:e15-e29.
27. Lam S, Boyle P, Healey GF, et al. EarlyCDT-Lung: an immunobiomarker test as an aid to early detection of lung cancer. *Cancer Prev Res (Phila)*. 2011;4:1126-1134.
28. Jett JR, Peek LJ, Fredericks L, Jewell W, Pingleton WW, Robertson JF. Audit of the autoantibody test, EarlyCDT(R)-lung, in 1600 patients: an evaluation of its performance in routine clinical practice. *Lung Cancer*. 2014;83:51-55.
29. Lowe FJ, Shen W, Zu J, et al. A novel autoantibody test for the detection of pre-neoplastic lung lesions. *Mol Cancer*. 2014;13:78.
30. Li S, Ma Y, Xiong Y, et al. Five tumor-associated autoantibodies expression levels in serum predict lung cancer and associate with poor outcome. *Transl Cancer Res*. 2019;8:1364-1373.
31. Pinato DJ, Howlett S, Ottaviani D, et al. Association of prior antibiotic treatment with survival and response to immune checkpoint inhibitor therapy in patients with cancer. *JAMA Oncol*. 2019;5(12):1774.
32. Murray A, Chapman CJ, Healey G, et al. Technical validation of an autoantibody test for lung cancer. *Ann Oncol*. 2010;21:1687-1693.
33. Scholten ET, Horeweg N, de Koning HJ, et al. Computed tomographic characteristics of interval and post screen carcinomas in lung cancer screening. *Eur Radiol*. 2015;25:81-88.

SUPPORTING INFORMATION

Additional supporting information may be found online in the Supporting Information section.

How to cite this article: Wang W, Zhuang R, Ma H, et al. The diagnostic value of a seven-autoantibody panel and a nomogram with a scoring table for predicting the risk of non-small-cell lung cancer. *Cancer Sci*. 2020;111:1699-1710. <https://doi.org/10.1111/cas.14371>